ORNL/TM-2023/3223

Behavior of Contaminants and Simulant Fission Products in the Advanced Chlorination Process

Joanna McFarlane
Breanna Vestal
Richard Mayes
Chasten Cobble
Matthew Vick
Kyoung Lee
Greg Westphal
Wesley Williams

December 2023

OAK RIDGE
National Laboratory

ORNL IS MANAGED BY UT-BATTELLE LLC FOR THE US DEPARTMENT OF ENERGY

DOCUMENT AVAILABILITY

Online Access: US Department of Energy (DOE) reports produced after 1991 and a growing number of pre-1991 documents are available free via https://www.osti.gov.

The public may also search the National Technical Information Service's National Technical Reports Library (NTRL) for reports not available in digital format.

DOE and DOE contractors should contact DOE's Office of Scientific and Technical Information (OSTI) for reports not currently available in digital format:

US Department of Energy
Office of Scientific and Technical Information
PO Box 62
Oak Ridge, TN 37831-0062
Telephone: (865) 576-8401
Fax: (865) 576-5728
Email: reports@osti.gov
Website: www.osti.gov

This report was prepared as an account of work sponsored by an agency of the United States Government. Neither the United States Government nor any agency thereof, nor any of their employees, makes any warranty, express or implied, or assumes any legal liability or responsibility for the accuracy, completeness, or usefulness of any information, apparatus, product, or process disclosed, or represents that its use would not infringe privately owned rights. Reference herein to any specific commercial product, process, or service by trade name, trademark, manufacturer, or otherwise, does not necessarily constitute or imply its endorsement, recommendation, or favoring by the United States Government or any agency thereof. The views and opinions of authors expressed herein do not necessarily state or reflect those of the United States Government or any agency thereof.

ORNL/TM-2023/3223

Nuclear Energy and Fuel Cycle Division

BEHAVIOR OF CONTAMINANTS AND SIMULANT FISSION PRODUCTS IN THE ADVANCED CHLORINATION PROCESS

Joanna McFarlane
Breanna Vestal
Richard Mayes
Chasten Cobble
Matthew Vick
Kyoung Lee
Greg Westphal
Wesley Williams

December 2023

Prepared by
OAK RIDGE NATIONAL LABORATORY
Oak Ridge, TN 37831-6283
managed by
UT-BATTELLE, LLC
for the
US DEPARTMENT OF ENERGY
under contract DE-AC05-00OR22725

CONTENTS

LIST OF FIGURES

LIST OF TABLES

ABSTRACT

The University of Tennessee, Knoxville and Oak Ridge National Laboratory have completed proof-of-principle testing on an advanced sulfur-based zirconium and aluminum chlorination process for the recovery of Zr or Al from spent fuel claddings and purification of the products. This process could be used to recover hafnium-free nuclear-grade zirconium for reuse or disposal as low-level waste. Testing showed that even non-optimized reaction protocols could produce zirconium product streams from simulated irradiated fuel with purities >90%. The chlorination process was tested on representative fission product species that would be found in Advanced Test Reactor fuel (ATR). First, fission product generation was determined through modeling and simulation of the ATR. The generation of fission products was used to selected contaminants and potentially volatile fission product simulants for laboratory testing. The goal is to identify which species may react with the sulfur-chlorine reagents and be transported into the advanced chlorination off-gas.

1. MODELING AND SIMULATION OF THE ADVANCED TEST REACTOR

Fuel from the Advanced Test Reactor (ATR) has been identified as a potential source for recovery of burnable actinides. Details on the geometry of ATR fuel and characteristics of burnup and enrichment are discussed in Hirschhorn (2023). The modeling activity started with a Monte Carle N-Particle (MCNP) simulation of the ATR to obtain the averaged neutron flux at sampling points within the reactor. It was necessary to use an averaged flux because of the complexity of the ATR geometry. Data obtained from sampling locations within the reactor were compared to calculations. Reactor performance parameters such as k_{eff} were also used to tune the model. Details on the model will be documented in a peer-reviewed publication (Lee et al., in preparation).

Once the flux profile was established, the ORIGEN code was used to calculate fission production from ^{235}U. These results are presented in

Table 1. The last column on the right, which shows grams of fission product per grams of U atom burned, provides the elemental ratios relevant to advanced chlorination processing.

Table 1. Radionuclides for consideration during advanced chlorination

Element	Isotopes and half-lives (>1 a)	Chloride (ΔG_f^0 kJ/mol @ 298 K)	Sulfide (ΔG_f^0 kJ/mol @ 298 K)	Abundance (relative to ΣFP from ^{235}U) [Sum for element in bold]
H	^{1}H – stable	HCl (-95.30)	H_2S (-33.329)	5.70×10^{-6}
	^{3}H – 12.32 a			6.37×10^{-4}
				$\Sigma = 6.42 \times 10^{-4}$
He	^{4}He – stable	Released during processing		**3.74×10^{-3}**
Ne	^{20}Ne – stable	Released during processing		**2.23×10^{-3}**
As	^{75}As – stable	$AsCl_3$ (-378.825)	As_2S_5	**1.02×10^{-6}**
Ge	^{76}Ge – stable	$GeCl_4$ (-466)	GeS_2 (-39.9)	**2.98×10^{-6}**
Se	^{77}Se – stable	$SeCl_2$		6.76×10^{-6}
	^{78}Se – stable			2.12×10^{-5}
	^{79}Se – 6.5e5 a			4.34×10^{-5}
	^{80}Se – stable			1.28×10^{-4}
	^{82}Se – stable			3.28×10^{-4}
				$\Sigma = 5.28 \times 10^{-4}$
Br	^{81}Br – stable	BrCl (-0.967)	S_2Br_2	**2.04×10^{-4}**
Kr	^{82}Kr – stable	Released during processing		2.69×10^{-6}
	^{83}Kr – stable			3.36×10^{-4}
	^{84}Kr – stable			1.22×10^{-3}
	^{85}Kr – 10.76 a			2.89×10^{-4}
	^{86}Kr – stable			2.02×10^{-3}
				$\Sigma = 3.87 \times 10^{-3}$
Rb	^{87}Rb – 4.88e10 a	RbCl (-405.8)	Rb_2S	**2.67×10^{-3}**
Sr	^{88}Sr – stable	$SrCl_2$ (-828.85)	SrS (-468.608)	3.76×10^{-3}
	^{90}Sr – 28.78 a			6.22×10^{-3}
				$\Sigma = 9.97 \times 10^{-3}$
Zr	^{96}Zr – stable	$ZrCl_4$ (-889.999)	ZrS_2	**8.86×10^{-2}**
Mo	^{95}Mo – stable	$MoCl_3$	MoS_2 (-267.156)	3.00×10^{-4}
	^{96}Mo – stable	$MoCl_5$	Mo_2S_3 (-395.654)	4.41×10^{-5}
	^{97}Mo – stable			7.29×10^{-3}
	^{98}Mo – stable			7.26×10^{-3}
	^{100}Mo – stable			8.07×10^{-3}
				$\Sigma = 2.30 \times 10^{-2}$
Tc	^{99}Tc – 2.13e5 a		TcS_2 (-216.1)	**6.69×10^{-3}**
			TcS_3 (-263)	
Ru	^{100}Ru – stable	$RuCl_4$		5.26×10^{-4}
	^{101}Ru – stable			6.61×10^{-3}
	^{102}Ru – stable			5.95×10^{-3}
	^{103}Ru – stable			3.04×10^{-3}
	^{104}Ru – stable			3.26×10^{-3}
				$\Sigma = 1.92 \times 10^{-2}$
Pd	^{104}Pd – stable		PdS (-93.688)	2.93×10^{-4}
	^{105}Pd – stable			4.37×10^{-4}
	^{106}Pd – stable			1.45×10^{-3}
	^{107}Pd – 6.5e6 a			6.21×10^{-4}
	^{108}Pd – stable			3.69×10^{-4}
	^{110}Pd – stable			1.28×10^{-4}
				$\Sigma = 3.30 \times 10^{-3}$
Ag	^{109}Ag – stable	AgCl (-109.764)	Ag_2S (-40.8)	**1.95×10^{-4}**

Table 1. Radionuclides for consideration during advanced chlorination (continued)

Element	Isotopes and half-lives (>1 a)	Chloride (ΔG_f^0 kJ/mol @ 298 K)	Sulfide (ΔG_f^0 kJ/mol @ 298 K)	Abundance (relative to ΣFP from ^{235}U) [Sum for element in bold]
Cd	^{110}Cd – stable	CdCl (-343.2)	CdS (-153.2)	4.90×10^{-5}
	^{111}Cd – stable			4.02×10^{-5}
	^{112}Cd – stable			3.58×10^{-5}
	^{113}Cd – stable			2.92×10^{-7}
	^{114}Cd – stable			5.49×10^{-5}
	^{116}Cd – 3e19 a			2.59×10^{-5}
				$\Sigma = 2.07 \times 10^{-4}$
In	^{115}In – 4.4e14 a	InCl (-164) $InCl_3$	In_2S_2 (142.158)	**1.28×10^{-5}**
Sn	^{115}Sn – stable	$SnCl_4$ (-457.7)	SnS (-108.2)	8.98×10^{-7}
	^{116}Sn – stable			6.40×10^{-6}
	^{117}Sn – stable			2.29×10^{-5}
	^{118}Sn – stable			2.02×10^{-5}
	^{119}Sn – stable			2.14×10^{-5}
	^{120}Sn – stable			2.21×10^{-5}
	^{121m}Sn – 55 a			1.71×10^{-6}
	^{121}Sn – stable			6.28×10^{-7}
	^{122}Sn – stable			2.83×10^{-5}
	^{123}Sn – stable			2.67×10^{-6}
	^{124}Sn – stable			4.92×10^{-5}
	^{126}Sn – 2.5e5			1.09×10^{-4}
				$\Sigma = 2.86 \times 10^{-4}$
Sb	^{125}Sb – 2.758 a	$SbCl_3$ (-322.5) $SbCl_5$ (-345.35)	Sb_2S_3 (-156.1)	**5.49×10^{-5}**
Te	^{126}Te – stable	$TeCl_4$ (-238.9)	TeS_2	3.38×10^{-6}
	^{128}Te – stable			7.02×10^{-4}
	^{130}Te – stable			3.07×10^{-3}
				$\Sigma = 3.77 \times 10^{-3}$
I	^{129}I – stable	ICl (-14.049)	S_2I_2	**8.29×10^{-4}**
Xe	^{128}Xe – stable	Released during processing		4.35×10^{-6}
	^{130}Xe – stable			6.19×10^{-5}
	^{131}Xe – stable			2.98×10^{-3}
	^{132}Xe – stable			7.59×10^{-3}
	^{134}Xe – stable			1.49×10^{-2}
	^{136}Xe – stable			2.24×10^{-2}
				$\Sigma = 4.49 \times 10^{-2}$
Cs	^{133}Cs – stable	CsCl (-414.36)		7.58×10^{-3}
	^{134}Cs – 2.065 a			6.60×10^{-4}
	^{135}Cs – 2.3e6 a			1.74×10^{-4}
	^{137}Cs – 30.07 a			1.09×10^{-2}
				$\Sigma = 1.93 \times 10^{-2}$
Ba	^{134}Ba – stable	$BaCl_2$ (-821.29)	BaS (-458.776)	6.13×10^{-6}
	^{136}Ba – stable			1.53×10^{-5}
	^{137}Ba – stable			1.49×10^{-5}
	^{138}Ba – stable			1.18×10^{-2}
				$\Sigma = 1.18 \times 10^{-2}$

Table 1. Radionuclides for consideration during advanced chlorination (continued)

Element	Isotopes and half-lives (>1 a)	Chloride (ΔG_f^0 kJ/mol @ 298 K)	Sulfide (ΔG_f^0 kJ/mol @ 298 K)	Abundance (relative to ΣFP from ^{235}U) [Sum for element in bold]
Lanthanides	^{139}La – stable	$LaCl_3$ (-1028.8)		**1.10×10^{-2}**
	^{140}Ce – stable	$CeCl_3$ (-983.9)		6.53×10^{-3}
	^{142}Ce – stable			1.09×10^{-2}
				$\Sigma = 1.74 \times 10^{-2}$
	^{141}Pr – stable	$PrCl_3$ (-1101.56)		**3.34×10^{-3}**
	^{142}Nd – stable	$NdCl_3$ (-1086.59)		5.39×10^{-2}
	^{143}Nd – stable			3.54×10^{-3}
	^{144}Nd – 2.36e15 a			3.67×10^{-3}
	^{145}Nd – stable			6.30×10^{-3}
	^{146}Nd – stable			6.30×10^{-3}
	^{148}Nd – stable			4.73×10^{-3}
				$\Sigma = 2.46 \times 10^{-2}$
	^{147}Pm – 2.62 a			**1.15×10^{-3}**
	^{147}Sm – 1.06e11 a	$SmCl_2$ (-857.148)		1.38×10^{-5}
	^{148}Sm – 6.3e15	$SmCl_3$ (1056.784)		1.65×10^{-4}
	^{149}Sm – stable			3.71×10^{-6}
	^{150}Sm – stable			2.01×10^{-3}
	^{151}Sm – 94.6 a			2.77×10^{-5}
	^{152}Sm – stable			1.03×10^{-3}
	^{154}Sm – stable			3.39×10^{-4}
				$\Sigma = 3.61 \times 10^{-3}$
	^{153}Eu – stable	$EuCl_2$ (-862.66)		5.95×10^{-4}
	^{154}Eu – 8.593 a	$EuCl_3$ (-976.846)		1.26×10^{-4}
	^{155}Eu – 4.7611 a			3.69×10^{-5}
				$\Sigma = 7.58 \times 10^{-4}$
	^{156}Gd – stable	$GdCl_3$ (1045.26)		8.72×10^{-5}
	^{158}Gd – stable			1.57×10^{-4}
	^{160}Gd – stable			2.75×10^{-6}
				$\Sigma = 2.46 \times 10^{-4}$
	^{159}Tb - stable	$TbCl_3$		**6.73×10^{-6}**
U	^{234}U, ^{235}U, ^{235m}U ^{236}U, ^{237}U, ^{238}U, ^{239}U	UCl_{30} (-823.8) UCl_4 (-962.3) UCl_6 (-1010)	Not included: depends on isotopic enrichment	
Np	^{237}Np, ^{238}Np, ^{239}Np, ^{240m}Np, ^{240}Np	$NpCl_4$ (-895.562)	Not included: depends on isotopic enrichment	
Pu	^{238}Pu, ^{239}Pu, ^{240}Pu, ^{241}Pu, ^{242}Pu, ^{243}Pu	$PuCl_4$ (-764.368)	Not included: depends on isotopic enrichment	
Am	^{241}Am, ^{243}Am	$AmCl_3$ (-905.105)	Not included: depends on isotopic enrichment	
Cm	^{244}Cm	$CmCl_3$	Not included: depends on isotopic enrichment	

2. METAL FISSION PRODUCT DISSOLUTION TESTING

To gain a better understanding of the chemistry of the fission products during chlorination, a variety of metals were exposed at various times and temperatures to S_2Cl_2. All reactions were performed under an inert N_2 atmosphere. Although exact product analysis was not preformed, the theoretical yields for each reaction were compared to the experimental yields given an assumed chlorination reaction, as seen in Eq. (1).

$$M + S_2Cl_2 \rightarrow MCl_x + S \tag{1}$$

The thermodynamic values for each reaction can be seen in **Error! Reference source not found.**. All reactions surveyed are thermodynamically favorable according to the free energy calculated. The early transition metals—Al, Ti, Zr, and Nb—have the more negative free-energy values, whereas the late transition metals—Ni, Ag, Re, and Pt—have more positive free-energy values.

Table 2. Thermodynamic values for the proposed chlorination of each metal with S_2Cl_2 according to the general Eq. (1) at 25°C (298 K) as calculated from NIST-JANAF tables

Metal	Metal chloride	Molar ΔG (kJ) at 25°C (298 K)
Al	$AlCl_3$	-570.82
Ti	$TiCl_4$	-658.89
Sn	$SnCl_4$	-379.39
Sn	$SnCl_2$ (by experiment, not formed in favor of $SnCl_4$)	-250.55
Zr	$ZrCl_4$	-811.13
Nb[a]	$NbCl_5$	-585.55
Fe	$FeCl_3$	-274.79
Re[a]	$ReCl_5$	-193.77
Cr	$CrCl_3$	-441.37
Mo[a]	$MoCl_5$	-324.95
Mo[a]	$MoCl_3$ (by experiment, not formed in favor of $MoCl_5$)	-266.56
Ni	$NiCl_2$	-219.34
Ag[a]	AgCl	-90.09
Pt[a]	$PtCl_2$	-53.98
Pd[a]	$PdCl_2$	Thermodynamic properties not found in literature
Te[a,b]	$TeCl_4$	-182.09
Cd[a,b]	$CdCl_2$	-304.05

[a] = Fission products

[b] = Future experiments

Following are summaries of the experiments performed to supplement the thermodynamic calculations presented in **Error! Reference source not found.**. Although all of the experiments have been performed, only the reactions of the fission products are presented.

2.1 MOLYBDENUM

A 1.5 g piece of Mo wire with unknown purity was obtained from the mechanics shop at the University of Tennessee in Knoxville. The metal was partially reacted after 28 h in refluxing (137°C) S_2Cl_2. There are two possible working equations for the chlorination of Mo using S_2Cl_2, as presented in Eqs. (2) and (3):

$$2\,Mo + 3\,S_2Cl_2 \rightarrow 2\,MoCl_3 + 6\,S \tag{2}$$

$$2\,Mo + 5\,S_2Cl_2 \rightarrow 2\,MoCl_5 + 10\,S \tag{3}$$

As seen in Figure 1, the solution became a deep blue color with a blue crystalline precipitate along the solvent line after reacting for 28 h, although the S_2Cl_2 solvent is deep yellow. The excess S_2Cl_2 solvent was removed, and a mass increase of 47% was observed.

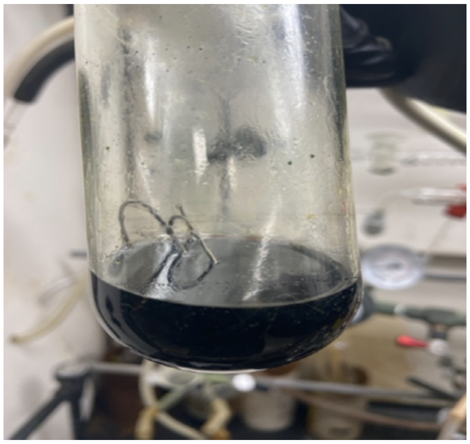

Figure 1. Mo wire after 28 h of reacting with S_2Cl_2.

Thionyl chloride was added in an effort to crystallize the solid residue from the reaction. A solid did crystallize, as seen in Figure 2, and single crystal x-ray diffraction was performed on the material. A crystal structure of the elemental sulfur byproducts from both chlorination reactions of Mo was observed.

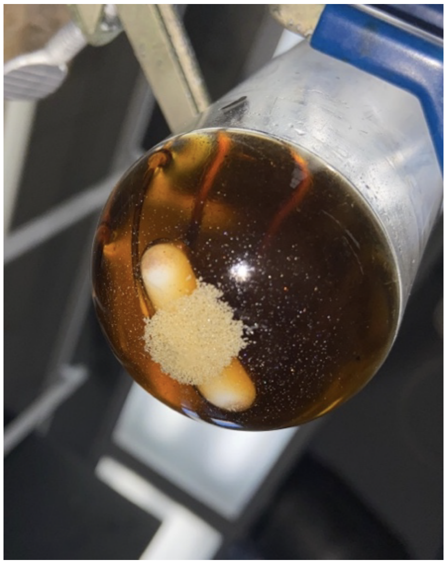

Figure 2. Reaction products after $SOCl_2$ was added to attempt a crystallization.

The blue material discovered from the chlorination of the Mo wire was not investigated further. The major finding from the experiment was that Mo metal reacts with S_2Cl_2.

2.2 SILVER

A small wire of Ag (0.534 g) was added to 10 mL (50× molar excess) of S_2Cl_2 and heated for a total of 3 h at 100°C. No visual evidence of reaction was observed. The volatile S_2Cl_2 was removed from the unreacted metal, and the mass of the Ag wire and any other nonvolatile solid was 0.536 g. Therefore, according to gravimetric and visual analysis, no reaction of Ag and S_2Cl_2 was observed.

Figure 3. Silver wire used in the chlorination reaction with S_2Cl_2.

2.3 IRON

A small wire of Fe (1.343 g) was added to 15.4 mL (5× molar excess) of S_2Cl_2 and heated to 150°C for 28 h. After the volatile excess solution was removed, the metal wire was not completely reacted (Figure 4), although a gain of 1.02 g was observed. According to the assumed reaction shown in Eq. (4), a 30% chlorination of Fe was observed.

$$2\,Fe + 3\,S_2Cl_2 \rightarrow 2\,FeCl_3 + 6\,S \tag{4}$$

Figure 4. Fe wire after chlorination with S_2Cl_2.

2.4 PLATINUM

A small wire of Pt (0.270 g) was added to 10 mL (90× molar excess) of S_2Cl_2 and heated to 100°C for a total of 3 h. No visual evidence of reaction was observed. The heating was stopped, but the metal was left in solution at room temperature overnight. No change was observed overnight. The volatile S_2Cl_2 was removed from the unreacted metal. The mass of the Pt wire and any other nonvolatile solid was 0.314 g, for a total mass gain of 0.044 g, or a 16% mass increase, or 31% chlorination according to the assumed Eq. (5).

$$Pt + S_2Cl_2 \rightarrow PtCl_2 + 2\,S \tag{5}$$

2.5 TIN

Tin granules (1.934 g, as seen in Figure 5) were added to 14.784 g (5.8 molar excess) of S_2Cl_2 at room temperature. The reaction was completed in approximately 5 min. The volatiles were removed from the product, and 2.161 g of solid remained. According to Eq. (6), the theoretical yield of nonvolatile materials for the assumed product of $SnCl_2$ is 4.134 g, whereas the theoretical yield according to the production of $SnCl_4$ is 2.089 g, as seen in Eq. (7). Therefore, gravimetric analysis of the reaction products is consistent with the production of $SnCl_4$, with an error of 3.44%.

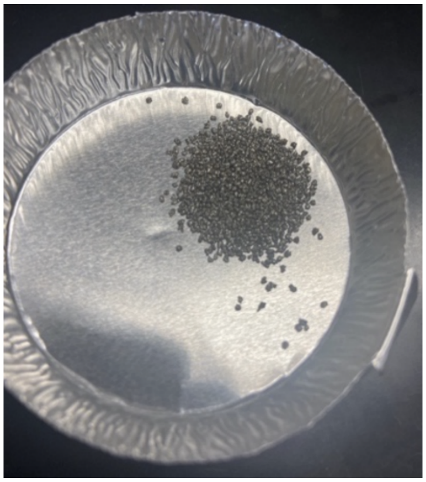

Figure 5. Tin granules prior to chlorination via S_2Cl_2.

$$Sn + S_2Cl_2 \rightarrow SnCl_2 + 2\,S \tag{6}$$
$$Sn + 2\,S_2Cl_2 \rightarrow SnCl_4 + 4\,S \tag{7}$$

2.6 PALLADIUM

A small sheet of thin Pd metal (0.111 g) was added to 10 mL (120× molar excess) of S_2Cl_2 and heated to 100°C for a total of 3 h. No visual evidence of reaction was observed. The volatile S_2Cl_2 was removed from the unreacted metal, and the mass of the Pd wire and any other nonvolatile solid was 0.116 g, for a total mass gain of 0.005 g, or 4% mass increase. Overall, very little reaction occurred between the Pd and S_2Cl_2 under the reaction conditions.

2.7 RHENIUM

A pellet of Re metal (2.772 g, Figure 6) was added to 10 mL (3.36× molar excess) of S_2Cl_2 and heated to 100°C for a total of 3 h. After only 30 min, the solution color darkened, and as heating continued heating, the darkening continued. However, after the 3 h of heating, the pellet was still present.

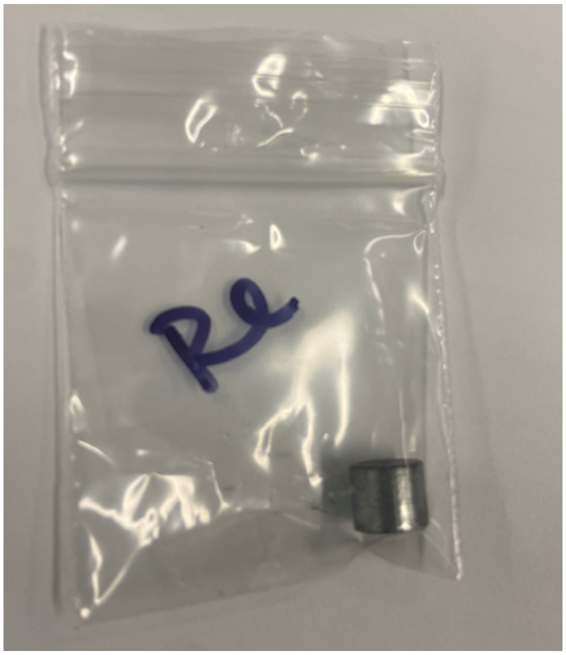

Figure 6. Re pellet.

The volatile S_2Cl_2 was removed from the remaining metal, and the mass of the rhenium pellet and chlorination products was 2.996 g, for a total mass gain of 0.224 g, or an 8% mass increase. However, there were obvious visual signs of reaction, with the assumed product of black $ReCl_5$ (Figure 7).

Figure 7. $ReCl_5$ produced from chlorination of the Re pellet via S_2Cl_2.

2.8 NIOBIUM

Niobium foil (2.296 g) was added to 21.16 g of S_2Cl_2 (3.1 excess). After no immediate reaction was observed, the solution was heated to 160°C for 3 h. After the S_2Cl_2 was removed from the metal, the mass of the material was consistent with 40% chlorination according to the proposed chlorination equation. However, the mass of the unreacted foil was 5.645 g (Figure 8), indicating a reaction of approximately 40% according to the proposed chlorination of Nb to form $NbCl_5$, as shown in Eq. (8).

Figure 8. Nb metal after 3 h of reaction in S_2Cl_2.

$$2\,Nb + 5\,S_2Cl_2 \rightarrow 2\,NbCl_5 + 10\,S \tag{8}$$

Additional S_2Cl_2 (24.91 g) was added back to the flask to continue chlorination, and the chlorination reaction was completed in 24 h. After drying, the yield of the products was 10.637 g, whereas the theoretical yield for the two nonvolatile products was 12.164 g, for an error of 14% according to Eq. (8).

3. CONCLUSIONS

A thermodynamic survey can be used to aid in predicting the general reactivity of fission products in advanced chlorination solvents. Early transition metals with very negative Gibbs free-energy values show a general affinity toward chlorination. Late transition metals and precious metals with higher but still negative Gibbs free-energy values do not chlorinate as easily. The rate of chlorination will depend on the surface area and the passivation of the surface by an oxide layer. Fission products will continue to be tested experimentally to affirm the calculated values for reactivity in the chlorinating solvent.

4. ACKNOWLEDGMENTS

The work was funded through the US Department of Energy Office of Nuclear Energy Materials Recovery and Waste Form Program (NE-43).

5. REFERENCES

Hirschhorn, J.A., McFarlane, J. (2023), *A Review of Advanced Test Reactor Fuel and Assessment of Its Compatibility with the ZIRCEX Chlorination Process*. ORNL/TM-2023/2882. doi:10.2172/1974319.

Lee, K., Westphal, G., Williams, W.C., McFarlane, J. (2024), *Fission Product Source by Simulation and Sampling of the Advanced Test Reactor* (in preparation).